Generalization of Double Illumination Method for Moiré Topography

Generalization of Double Illumination Method for Moiré Topography

Sadahiko NAGAE*, Hiroko MATSUOKA** and Masaru MATSUO***

(Recieved November 15, 1981)

Generalization of the doudle illumination method by two light sources in moiré topography is discussed, and the three dimensional analysis of its mathematical basis is developed for the following two cases: In one case the grating has a light intensity distribution expressed by a fundamental harmonic wave, and in the other case it has a light intensity distribution expressed by a periodic function with many components.

The characteristics of the two cases are considered theoretically and several examples of the moiré fringe patterns observed by the double illumination method are presented.

1. Introduction

The method of Surface Contours[1] and Moiré Topography[2], which were first conceived by D. M. Meadows *et al* and H. Takasaki independently, are excellent and ingenious ways to observe contour lines of three dimensional objects. The both techniques use a grating placed in front of an object to be tested, and compose interference fringes called *moiré* by superimposing the original grating upon its shadow grating casted onto the surface of the object. These methods have the following merits: Firstly, they do not need any special coherent light sources such as a laser, and the resultant moiré patterns themselves give the contours directly displaying the depth of the surface from the plane of the grating screen. Secondly, the required experimental set up is enough to use common apparatuses such as a 35 mm film loaded camera, standard slide projector, hand-made plane grating, and so on. Thirdly, the depth interval between successive moiré fringes has a practical precision.

Applications of these methods, however, are limited within the size up to a living body, because it is difficult to make a grating screen with such a big size to cover the body, keeping the grating lines straight and tight enough so that all the lines of the screen should always have a good spacing and should be parallel. To cover the demerit, M. Suzuki *et al*[3] and Yoshizawa *et al*[4] independendently proposed another method to derive the same kind of contour line, using moiré interference fringes produced by a shadow grating projected on the object and the original graing placed in front of a film loaded in a camera. The principle itself is almost the same as that mentioned above, but a large field of applications is possible because of the projecting system which can cover a bigger object. The necessary equipment for this technique is not as simple as in the former methods, however the resultant information is wider than that in the previously described technique.

* Course of Mathematics and Related Fields, College of Integrated Arts and Sciences.

** Graduate Student, Department of Clothing Science, Faculty of Home Economics, Nara Women's University.

*** Department of Clothing Science, Faculty of Home Economics, Nara Women's University.

On the other hand, J. D. Hovanesian *et al*[5] advanced the latter method to extract subtractive deformations alone from moiré patterns, by usind a half mirror to overlap the image of the original object onto the object after being deformed.

Sometimes the former techniques by Meadows and Takasaki are called "*The Solid Grating Type*" and the latter techniques by Suzuki, Yoshizawa and Hovanesian are called "*The Projected Grating Type*". The both methods are widely used in these days not only in the fields of general engineering needs[6], but also of measuring human bodies from medical needs[7], and designing clothes from textile or cloth-manufacturing needs[8]. S. Nagae *et al* have applied these moiré techniques to the fields of Descriptive Geometry, where arbitrary sections of a solid body and intersecting lines of more than two solid bodies were obtained successfully[9~10]. The theory is based on that the contour lines by moiré methods correspond to the index projected lines in Descriptive Geometry when certain experimental conditions are satisfied[11]. In these methods it is essential to obtain; (i) a good visibility of the contour lines in greater depths of the object, (ii) shadow-free, high contrast images, and (iii) a narrow line width of the moiré fringes.

The papers by D. M. Meadows *et al*[1] and H. Takasaki[2] refered to a two point light source method as one of the expanded techniques to obtain shadow-free photographs, however, any rigorous analysis on the method was not given. One of the main reasons seems to be technical difficulties, for example, the difficulty in setting the two light sources symmetrically to the observation point to obtain a good visibility and contrast.

This paper describes a technique to diminish the experimental handicap, after showing a mathematical analysis extended from two dimensional treatment to three dimensional one.

2. Principle and Method

The light intensity distribution transmitted from an original grating screen can be regarded as a carrier wave in communication theory, and the light intensity distribution due to its shadow grating which is formed, by projection, on the surface of the object can be regarded as a phase modulated wave. It can be said that another grating carrying an information about the surface geometry of the object is generated from the original grating by the projection. Therefore, moiré fringes are resulted from the interference between the original and shadow gratings. The counter lines in the moiré pattern correspond to a demodulated wave to give the information of the surface geometry, though often buried in various noises such as unwanted aliasing moiré fringes, high harmonics' waves from the original grating, and so on.

In this section, the two-source method is developed to obtain a shadow-free, high contrast moiré pattern of the object under test, and two cases are mathematically treated; one is a case of a grating with transmittace of a fundamental harmonic wave ($n = 1$), and another is a case of a grating with transmittance of high harmonics' waves ($n \to \infty$). The technical methods for designing the grating will be described on the two cases in the solid grating type arrangement.

2.1 Grating having fundamental harmonic transmittance

In Fig. 1, the x and y axes are taken perpendicular and parallel to the lines of the plane grating screen (G) respectively, whereas the z axis is taken along the normal to the screen surface. Two light sources (S_1) and (S_2), and an observation point (C) are on a line parallel to the plane of the screen and separated by distance h from it. Let the first light source (S_1) be on the z axis, and the observation point (C) be separated by distances d_1 and d_2, respectively from the light sources (S_1) and (S_2). And let the initial position of the screen, which is displaced along the x-y plane during observation, is to be at a distance ϵ from the origin (O) in the direction of the x axis. The object to be tested is placed on the opposite side of the grating screen to the light sources.

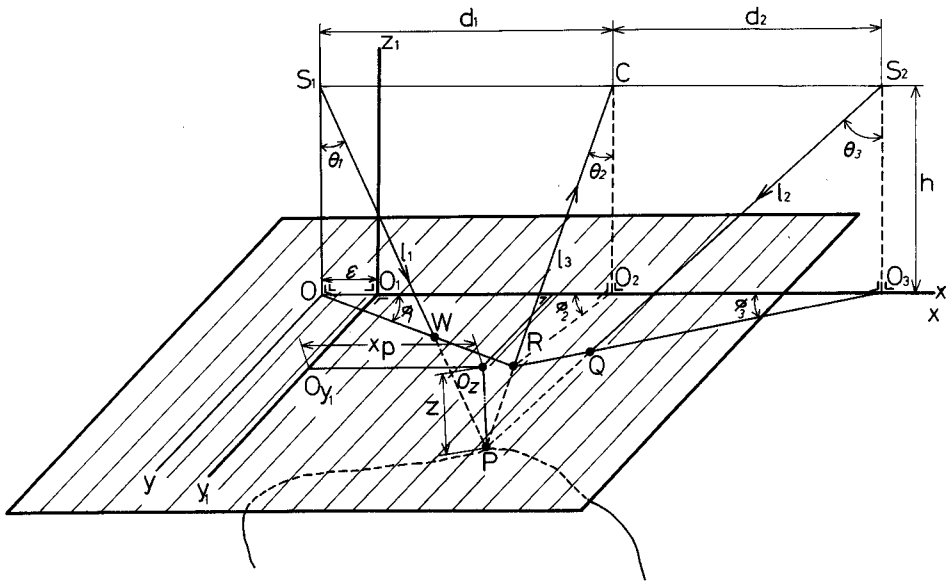

Fig. 1. Schematic representation of two-source method in moiré topotraphy. The letters (W), (R) and (Q) are the points in plane on the surface of the grating, with which the lines $\overline{S_1P}$, $\overline{CP}$ and $\overline{S_2P}$ are intersected. The letter x_p is a distance from the point (O_{y_1}) to the point (O_z), which is right above the point (P) on the surface of an object and an intersecting point where the perpendicular line $\overline{PO_z}$ meets with the plane of the grating. The depth of the point (P) from the plane is z, which is taken positive to downward.

When the surface of the object is illuminated through the grating by a point source (S_1), the projecteds shadow grating is formed on the surface. Then, the light intensity in the small surface area around a point (P) is described as[1)],

$$I_1(x, y) \propto \left[\frac{1}{2} + \frac{1}{2} \sin\left\{ \frac{2\pi}{p'} (x_P + \epsilon) / \cos\phi_1 - \frac{2\pi}{p_0'} z \tan\theta_1 \right\} \right] . \quad (1)$$

If the period of the sinusoidal wave, i.e., the grating constant be p_0, the corresponding period of the grating in the $\overline{WO}$ direction is $p_0' = p_0/\cos\phi_1$, and further the period of the

shadow grating around the point (P) can be obtained as

$$p' = \{ (h+z)\, p_0 / h \cos\phi_1 \}, \tag{2}$$

by a simple geometrical consideration.

Here it is noted that the sources are not collimated so that the period of the shadow grating must increase as the distance from the screen increases. If the surface area around the point (P), illuminated by the first light source (S_1) alone, is observed through the screen, the intensity distribution found by the eye or on a film at the point (C) will be the product of the intensity transmittance in Eq. (1), and the intensity transmittance of the original grating.

Namely,

$$I_{S_1} = \frac{I \cos\psi_1 (x,y,z)}{r_1^2 (x,y,z)} \left[\frac{1}{2} + \frac{1}{2} \sin\left\{ \frac{2\pi}{p'} \times (x_P + \epsilon) / \cos\phi_1 - \frac{2\pi}{p_0'} z \tan\theta_1 \right\} \right]$$
$$\times \left[\frac{1}{2} + \frac{1}{2} \sin\left\{ \frac{2\pi}{p''} (x_P + \epsilon) / \cos\phi_2 + \frac{2\pi}{p_0''} z \tan\theta_2 \right\} \right], \tag{3}$$

where the period of the original grating in the $\overline{O_2R}$ direction is $p_0'' = p_0/\cos\phi_2$, and the period of the shadow graing arround the point (P), viewed from the point (C) is given as

$$p'' = \{ (h+z)\, p_0 / h \cos\phi_2 \}. \tag{4}$$

In Eq. (3), I is the light intensity of the source (S_1) emitted onto the small area around the point (P), $\psi_1(x,y,z)$ is the angle between the incident ray (l_1) and the surface normal at the point (P), and $r_1\,(x,y,z)$ is the distance from the source (S_1) to the point (P).

Then, Eq. (3) becomes

$$I_{S_1} = \frac{I \cos\psi_1 (x,y,z)}{r_1^2 (x,y,z)} \left[\frac{1}{2} + \frac{1}{2} \sin\left\{ \frac{2\pi h}{p_0 (h+z)} (x_P + \epsilon) - \frac{2\pi}{p_0} z \tan\theta_1 \cos\phi_1 \right\} \right] \times \left[\frac{1}{2} + \frac{1}{2} \sin\left\{ \frac{2\pi h}{p_0 (h+z)} \times (x_P + \epsilon) + \frac{2\pi}{p_0} z \tan\theta_2 \cos\phi_2 \right\} \right] \tag{5-a}$$

$$= K_1 \left[1 + \sin\left\{ \frac{2\pi h}{p_0 (h+z)} (x_P + \epsilon) - \frac{2\pi}{p_0} z \tan\theta_1 \cos\phi_1 \right\} + \sin\left\{ \frac{2\pi h}{p_0 (h+z)} (x_P + \epsilon) + \frac{2\pi}{p_0} z \tan\theta_2 \cos\phi_2 \right\} - \frac{1}{2} \cos\left\{ \frac{4\pi h}{p_0 (h+z)} (x_P + \epsilon) + \frac{2\pi z}{p_0} (\tan\theta_2 \cos\phi_2 - \tan\theta_1 \cos\phi_1) \right\} + \frac{1}{2} \cos\frac{2\pi z}{p_0} \left\{ (\tan\theta_1 \cos\phi_1 + \tan\theta_2 \cos\phi_2) \right\} \right], \tag{5-b}$$

where $K_1 = I \cos \psi_1 (x, y, z) / 2r_1^2 (x, y, z)$ is taken as a constant by assuming that the slopes of the surface vary only slowly and $\cos \psi_1 (x, y, z)$ is substantially constant, irrespectively of the position of (P), over an appreciable area of the surface.

When the surface around the point (P) is illuminated only by the second light source (S_2) through the grating and is observed again through the grating, the intensity distribution will be given similarly by

$$I_{S_2} = \frac{I \cos \psi_2 (x, y, z)}{r_2^2 (x, y, z)} \left[\frac{1}{2} + \frac{1}{2} \sin \left\{ \frac{2\pi h}{p_0 (h+z)} \times (x_P + \epsilon) + \frac{2\pi}{p_0} z \tan \theta_3 \cos \phi_3 \right\} \right] \times \left[\frac{1}{2} + \frac{1}{2} \sin \left\{ \frac{2\pi h}{p_0 (h+z)} (x_P + \epsilon) + \frac{2\pi}{p_0} z \tan \theta_2 \cos \phi_2 \right\} \right] . \quad (6\text{-a})$$

That is,

$$I_{S_2} = K_2 \left[1 + \sin \left\{ \frac{2\pi h}{p_0 (h+z)} (x_P + \epsilon) + \frac{2\pi}{p_0} z \tan \theta_3 \cos \phi_3 \right\} + \sin \left\{ \frac{2\pi h}{p_0 (h+z)} (x_P + \epsilon) + \frac{2\pi}{p_0} z \tan \theta_2 \cos \phi_2 \right\} - \frac{1}{2} \cos \left\{ \frac{4\pi h}{p_0 (h+z)} (x_P + \epsilon) + \frac{2\pi z}{p_0} (\tan \theta_3 \cos \phi_3 + \tan \theta_2 \cos \phi_2) \right\} + \frac{1}{2} \cos \left\{ \frac{2\pi z}{p_0} (\tan \theta_3 \cos \phi_3 - \tan \theta_2 \cos \phi_2) \right\} \right] , \quad (6\text{-b})$$

where $K_2 = I \cos \psi_2 (x, y, z) / 2r_2^2 (x, y, z)$ is a constant.

On the other hand, the following relations will be derived by a simple geometrical consideration (see Fig. 1).

$$\tan \theta_1 \cos \phi_1 + \tan \theta_2 \cos \phi_2 = d_1 / (h+z) , \quad (7)$$

and

$$\tan \theta_3 \cos \phi_3 - \tan \theta_2 \cos \phi_2 = d_2 / (h+z) . \quad (8)$$

To return to Eqs. (5-b) and (6-b), the first term is a D. C. (bias) component that gives a constant light intensity contributing to the back ground, and the high harmonics terms containing ϵ should be averaged out of the expression if the screen is moved along its plane in the direction of the x axis, during observation, as Meadows and Takasaki pointed out. Finally, the last cosine terms represent the moiré patterns by the first and second light sources (S_1) and (S_2) formed for the small area around the point (P).

By substituting Eqs. (7) and (8) to the last cosine terms mentioned above and considering that the maximum and minimum of the terms correspond to the bright and dark

fringes of the moiré patterns, the following equations can be derived,

$$\frac{2\pi d_1 z_{S_1}}{p_0 (h + z_{S_1})} = 2\pi N \qquad \text{then} \qquad z_{S_1} = \frac{hN}{d_1/p_0 - N} , \tag{9-a}$$

and

$$\frac{2\pi d_2 z_{S_2}}{p_0 (h + z_{S_2})} = 2\pi N \qquad \text{then} \qquad z_{S_2} = \frac{hN}{d_2/p_0 - N} , \tag{9-b}$$

where N is an integer to specify the order of the fringe lines. Thus the N-th fringe line gives an equal depth line. It is evident that the two moiré patterns described by Eqs. (5) and (6) coinside if the condition $d_1 = d_2 = d$ holds. That is, exact doubling of the countors can be realized by using two light sources arranged symmetrically about the observation point (C). To obtain a good visibility of the moiré fringes with this two-source system, however, it is very important to set the two offset projectors exactly in the symmetrical position. When this condition is satisfied, the moiré pattern obtained with simultaneous illumination has the sum of the light intensity, I_{S_1} and I_{S_2} .

On the other hand, it is possible to obtain the intensity multiplication $I_{S_1} \times I_{S_2}$ by taking the pictures of the images under separated exposures and then superimosing two negative films of the moiré patterns.

Corresponding to Eqs. (5-b) and (6-b), the intensity distributions of the moiré fringes observed under separated exposures are

$$I_{S_1} \sim \frac{K_1'}{2} \left\{ 1 + \cos \frac{2\pi}{p_0} \left(\frac{dz}{h + z} \right) \right\} , \tag{10-a}$$

and

$$I_{S_2} \sim \frac{K_2'}{2} \left\{ 1 + \cos \frac{2\pi}{p_0} \left(\frac{dz}{h + z} \right) \right\} . \tag{10-b}$$

If the photographs are taken under the same conditions, the two constants K_1' and K_2' should be $K_1' = K_2' = K'$.

Therefore, for the case of the intensity sum, $I_S = I_{S_1} + I_{S_2}$,

$$I_S \sim K' \left\{ 1 + \cos \frac{2\pi}{p_0} \left(\frac{dz}{h + z} \right) \right\} \tag{11}$$

and for the case of the intensity multiplication, $I_S' = I_{S_1} \times I_{S_2}$,

$$I_S' \sim \frac{K'^2}{4} \left\{ 1 + \cos \frac{2\pi}{p_0} \left(\frac{dz}{h + z} \right) \right\}^2 . \tag{12}$$

In Fig. 2, the intensity curves are shown for I_S, I_S' and $2 \times I_S'$ respectively, where the vertical axis is proportional to the intensity level and the abscissa is taken as $f(z) = 2dz / p_0 (h + z)$. Therefore the moiré fringe visibility becomes better under the multiplica-

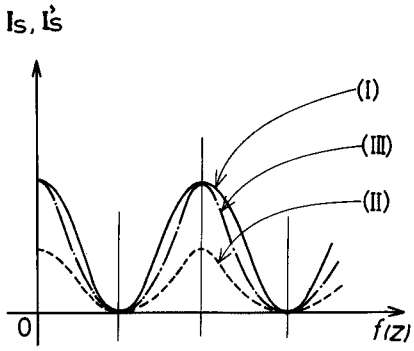

Fig. 2. Intensity curves in moiré fringes, (I) for I_S, (II) for I'_S and (III) for $2 \times I'_S$, respectively.

tion $I'_S = I_{S_1} \times I_{S_2}$, if the transmittance of the used screen is supposed to be a form of the fundermental wave.

2.2 Grating having higher harmonics transmittance

In the section 2.1, the contour lines formed by a sinusoidal grating with only the fundamental component has been analyzed. In this section, disscussion will be given on the contour lines formed by a grating whose light transmittance has many higher harmonics components.

When the surface of the object is illuminated by the two point sources, through the grating having a transmittance expressed by an arbitrary periodic function, and observed from the point (C), through the grating, the intensity distribution found for the surface area around the point (P) is expressed as,

$$I_{S_1} = C_1 \left[1 + g \left\{ \frac{2\pi h}{p_0 (h+z)} x - \frac{2\pi}{p_0} z \tan\theta_1 \cos\phi_1 \right\} \right] \times \left[1 + g \left\{ \frac{2\pi h}{p_0 (h+z)} x + \frac{2\pi}{p_0} z \tan\theta_2 \cos\phi_2 \right\} \right], \tag{13}$$

$$I_{S_2} = C_2 \left[1 + g \left\{ \frac{2\pi h}{p_0 (h+z)} x + \frac{2\pi}{p_0} z \tan\theta_3 \cos\phi_3 \right) \right\} \right] \times \left[1 + g \left\{ \frac{2\pi h}{p_0 (h+z)} x + \frac{2\pi}{p_0} z \tan\theta_2 \cos\phi_2 \right) \right\} \right], \tag{14}$$

where in comparison with Eqs. (5-b) and (6-b), $x = x_p + \epsilon$, and the constants of C_1 and C_2 are $C_1 = 2K_1$ and $C_2 = 2K_2$, respectively.

The arbitrary function $g(x)$ expressing the transmittance of the grating can be expanded into the following Fourier series;

$$g(x) = \sum_{n=1}^{\infty} (a_n \sin nx + b_n \cos nx) . \tag{15}$$

By substituting Eq. (15) into Eqs. (13) and (14), the light intensities become

$$
\begin{aligned}
I_{S_1} = C_1 < 1 + \sum_{n=1}^{\infty} \Bigg[& a_n \sin\left\{ \frac{2\pi n}{p_0} \left(\frac{hx}{h+z} - z \tan\theta_1 \cos\phi_1 \right) \right\} \\
& + b_n \cos\left\{ \frac{2\pi n}{p_0} \left(\frac{hx}{h+z} - z \tan\theta_1 \cos\phi_1 \right) \right\} \Bigg] \\
& + \sum_{n=1}^{\infty} \Bigg[a_n \sin\left\{ \frac{2\pi n}{p_0} \left(\frac{hx}{h+z} + z \tan\theta_2 \cos\phi_2 \right) \right\} \\
& + b_n \cos\left\{ \frac{2\pi n}{p_0} \left(\frac{hx}{h+z} + z \tan\theta_2 \cos\phi_2 \right) \right\} \Bigg] \\
& + \frac{1}{2} \sum_{n=1}^{\infty} \Bigg[\left(a_n^2 + b_n^2 \right) \cos\left\{ \frac{2\pi n d_1 z}{p_0 (h+z)} \right\} \\
& + \left(b_n^2 - a_n^2 \right) \cos\left\{ \frac{2\pi n}{p_0} \left(\frac{2hx}{h+z} + z \tan\theta_2 \cos\phi_2 - z \tan\theta_1 \cos\phi_1 \right) \right\} \\
& + a_n b_n \sin\left\{ \frac{2\pi n}{p_0} \left(\frac{2hx}{h+z} + z \tan\theta_2 \cos\phi_2 - z \tan\theta_1 \cos\phi_1 \right) \right\} \Bigg] \\
& + \sum_{\substack{m=1 \\ (m \neq n)}}^{\infty} \sum_{n=1}^{\infty} \left(b_m b_n - a_m a_n \right) \cos\Bigg[\frac{2\pi}{p_0} \Bigg\{ \frac{(m+n)hx}{h+z} \\
& \qquad + z \left(m \tan\theta_2 \cos\phi_2 - n \tan\theta_1 \cos\phi_1 \right) \Bigg\} \Bigg] \\
& + \left(a_m a_n + b_m b_n \right) \cos\Bigg[\frac{2\pi}{p_0} \Bigg\{ \frac{(n-m)hx}{h+z} - z \left(n \tan\theta_1 \cos\phi_1 \right. \\
& \left. + m \tan\theta_2 \cos\phi_2 \right) \Bigg\} \Bigg] + \left(a_m b_n + a_n b_m \right) \sin\Bigg[\frac{2\pi}{p_0} \Bigg\{ \frac{(n+m)hx}{h+z} \\
& - z \left(n \tan\theta_1 \cos\phi_1 - m \tan\theta_2 \cos\phi_2 \right) \Bigg\} \Bigg] + \left(a_m b_n - a_n b_m \right) \sin\Bigg[\frac{2\pi}{p_0} \\
& \left\{ \frac{(m-n)hx}{h+z} + z \left(n \tan\theta_1 \cos\phi_1 + m \tan\theta_2 \cos\phi_2 \right) \right\} \Bigg] >, \qquad (16)
\end{aligned}
$$

and

$$I_{S_2} = C_2 < 1 + \sum_{n=1}^{\infty} \left[a_n \sin \left\{ \frac{2\pi n}{p_0} \left(\frac{hx}{h+z} - z \tan \theta_3 \cos \phi_3 \right) \right\} \right.$$

$$\left. + b_n \cos \left\{ \frac{2\pi n}{p_0} \left(\frac{hx}{h+z} - z \tan \theta_3 \cos \phi_3 \right) \right\} \right]$$

$$+ \sum_{n=1}^{\infty} \left[a_n \sin \left\{ \frac{2\pi n}{p_0} \left(\frac{hx}{h+z} + z \tan \theta_2 \cos \phi_2 \right) \right\} \right.$$

$$\left. + b_n \cos \left\{ \frac{2\pi n}{p_0} \left(\frac{hx}{h+z} + z \tan \theta_2 \cos \phi_2 \right) \right\} \right]$$

$$+ \frac{1}{2} \sum_{n=1}^{\infty} \left[(a_n^2 + b_n^2) \cos \left\{ \frac{2\pi n d_2 z}{p_0 (h+z)} \right\} \right.$$

$$+ (b_n^2 - a_n^2) \cos \left\{ \frac{2\pi n}{p_0} \left(\frac{2hx}{h+z} + z \tan \theta_2 \cos \phi_2 + z \tan \theta_3 \cos \phi_3 \right) \right\}$$

$$\left. + a_n b_n \sin \left\{ \frac{2\pi n}{p_0} \left(\frac{2hx}{h+z} + z \tan \theta_2 \cos \phi_2 + z \tan \theta_3 \cos \phi_3 \right) \right\} \right]$$

$$+ \sum_{\substack{m=1 \\ (m \neq n)}}^{\infty} \sum_{n=1}^{\infty} \left[(b_m b_n - a_m a_n) \cos \left[\frac{2\pi}{p_0} \left\{ \frac{(m+n) hx}{h+z} \right. \right. \right.$$

$$\left. \left. \left. + z (m \tan \theta_2 \cos \phi_2 + n \tan \theta_3 \cos \phi_3) \right\} \right] \right.$$

$$+ (a_m a_n + b_m b_n) \cos \left[\frac{2\pi}{p_0} \left\{ \frac{(n-m) hx}{h+z} - z (m \tan \theta_2 \cos \phi_2 \right. \right.$$

$$\left. \left. - n \tan \theta_3 \cos \phi_3) \right\} \right]$$

$$+ (a_m a_n + b_m b_n) \sin \left[\frac{2\pi}{p_0} \left\{ \frac{(m+n) hx}{h+z} - z (m \tan \theta_2 \cos \phi_2 \right. \right.$$

$$\left. \left. - n \tan \theta_3 \cos \phi_3) \right\} \right]$$

$$+ (a_n b_m - a_m b_n) \sin \left[\frac{2\pi}{p_0} \left\{ \frac{(n-m) hx}{h+z} \right. \right.$$

$$\left. \left. \left. + z (n \tan \theta_3 \cos \phi_3 - m \tan \theta_2 \cos \phi_2) \right\} \right] \right] > . \qquad (17)$$

Again, the terms which represent the moiré patterns around the point (P) on the surface are obtained after averaging out other terms,

$$I_{S_1} \sim C_1 \left[1 + \frac{1}{2} \sum_{n=1}^{\infty} (a_n^2 + b_n^2) \cos \left\{ \frac{2\pi n d_1 z}{p_0 (h+z)} \right\} \right], \tag{18}$$

and

$$I_{S_2} \sim C_2 \left[1 + \frac{1}{2} \sum_{n=1}^{\infty} (a_n^2 + b_n^2) \cos \left\{ \frac{2\pi n d_2 z}{p_0 (h+z)} \right\} \right]. \tag{19}$$

Clearly, the two moiré patterns by the two light sources coinside if the condition $d_1 = d_2 = d$ holds. Moreover, when the photographs are taken under precisely the same conditions, the two constants C_1 and C_2 should be the same, $C_1 = C_2 = C$. Then, the intensities should become $I_{S_1} = I_{S_2} = I_S$,

$$I_S \sim C \left[1 + \frac{1}{2} \sum_{n=1}^{\infty} (a_n^2 + b_n^2) \cos \frac{2\pi}{p_0} \left(\frac{ndz}{h+z} \right) \right]. \tag{20}$$

The intensity distribution of the moiré pattern, I_S is expressed by a Fourier series whose coefficients are the square of the coefficients in the intensity transmittance of the grating. Suppose that the intensity transmittance is given by a square wave,

$$g(x) = \begin{cases} 1 \ ; \text{ for } \ (mp_0 + \delta/2) \geq x \geq (mp_0 - \delta/2), \ m = 1, 2, 3, \ldots \\ 0 \ ; \text{ for } \ \textit{else where} \end{cases}$$

where δ ($< p_0$) is the slit width. Then, the coefficients a_n and b_n become

$$a_n = \frac{2\delta}{p} \operatorname{sinc} \left(n \frac{\delta}{p_0} \pi \right), \quad b_n = 0 \tag{21}$$

Except for the case of $\delta \fallingdotseq p_0$, a_n must diminish rapidly with increasing n along the envelope of the sinc-function. This tendency is more intensified for the square of the coefficients and thus the moiré intensity distribution given by Eq. (20) becomes closer to that in Eq. (11) or (12).

For practical use, the slit width δ is taken in the range $(1/5)p_0 \sim (4/5)p_0$. Numerical computations indicate that both the contrast and visibility evaluated from Eqs. (20) and (21) are worse than those obtained with Eq. (11) or (12). Therefore, the grating having the fundamental sinusoidal wave transmittance is better in use for the moiré topography.

3. Experiment

In the present study, two 100 watt projector lamps were placed at an equal distance, 90 cm from the camera, which was directed to the center of the plane grating screen with its axis along the normal to the screen. The distance between the camera and the screen was varied depending upon the size of the object to be tested. In general, it is known

that the smaller the size of the light source is, the sharper the contrast of the bright and dark strips become. But a source too small in size is not always recommended, because it will not give enough illumination required for taking photographs. A variable pin hole, 0.5 ~ 3 mm in diameter, was placed at the focal point of the condenser lens of the projector, and this pin hole was regarded as a practical light source.

The object was placed behind the grating at a proper distance. The frame of the screen was made of an iron angle, 1.5 m in width and 1.2 m in height. The grating lines were constructed with black nylon strings. Both ends of the strings were fixed with iron rod-screws onto the iron flame to stretch them in desired parallelity and spacing. The spacing of the grating was 2 mm, whereas the diameter of the strings was 0.8 mm.

3.1 In Case of Simple Models

Photo. 1 shows a right cone model of 20 cm height contoured by the system described above, where Photo. 1 (a) is by the illumination (I_{S_1}) from the source (S_1), and Photo. 1 (b) is by the illumination (I_{S_2}) from the source (S_2). The main distances of the experimental set up are $p_0 = 2$ mm, $d_1 = d_2 = 90$ cm, and $h = 105$ cm, with the depth difference between succesive fringes as small as $\Delta z = 2.3$ mm. The aperture of the camera lens should be kept small to have an enough forcal depth. The exposures were about 4 seconds with an ASA 400 film and aperture $f/22$.

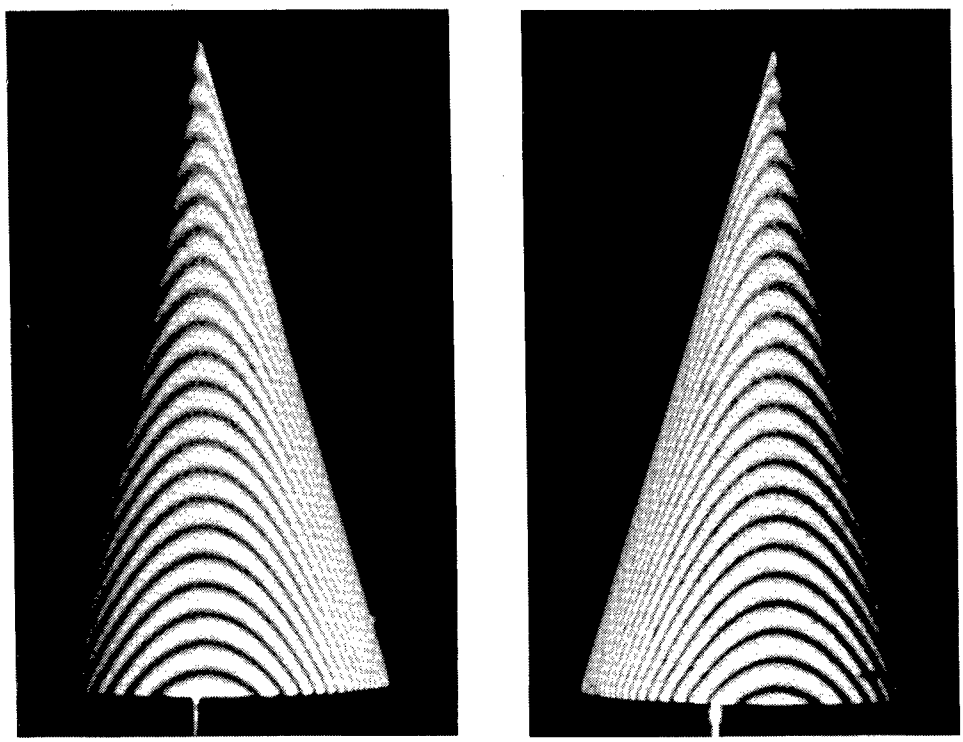

(a) (b)

Photo. 1. Contouring lines of a right cone model, where (a) is by I_{S_1} and (b) is by I_{S_2}.

Photo. 2 shows the same model observed under double illumination, the exposure time being one half of that in Photo. 1. Photo. 2 (a) is the result of the simultaneous illumination, while Photo. 2 (b) is the result of the alternate illumination. The former was taken by a single exposure under simultaneous illuminations (I_{S_1}) and (I_{S_2}), and the latter was taken on a film under successive exposures, firstly by the illumination (I_{S_1}) alone, and secondly by the illumination (I_{S_2}) alone. It is seen that the moiré fringes in the two photographs are identical. The symmetry of the double illuminating was always confirmed by such coincidence of the moiré patterns obtained under the simultaneous and alternative illuminations.

In comparison with Photo. 1, it is clear that the patterns in Photo. 2 are free from shadow. Further, the observed fringes are sharper than in Photo. 1, and keep enough visibility.

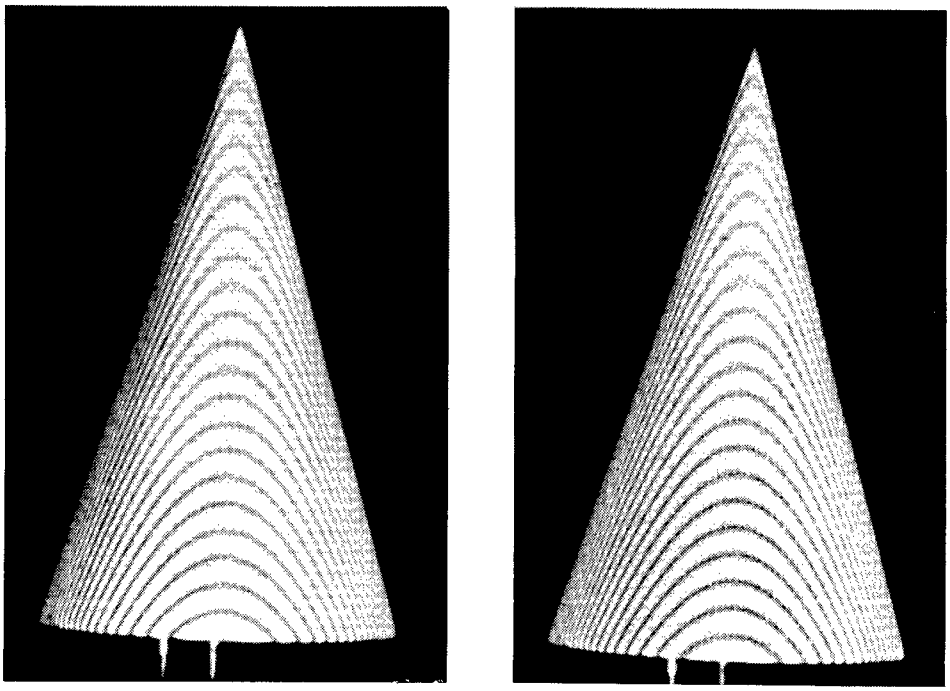

(a) (b)

Photo. 2 Contouring lines of the same model as shown in the Photo. 1, where (a) is taken with simultaneous illumination; I_{S_1} and I_{S_2}, and (b) is taken with alternate illumination; I_{S_1} or I_{S_2}.

Photo. 3 shows intersecting bodies consisting of the right cone used above and a cylinder that crosses at right angle. The experimental conditions were the same as those for Photo. 2. Photo. 3 (a) is a case that the cylinder pierces the cone, while Photo. 3 (b) is a case that the cone pierces the cylinder. The moiré fringes formed on each surface of the corn and cylinder with common numbers $N = 1, 2, 3, \ldots$ correspond to equi-depth lines on the surfaces and are encountered with each other on the inter-section line, as

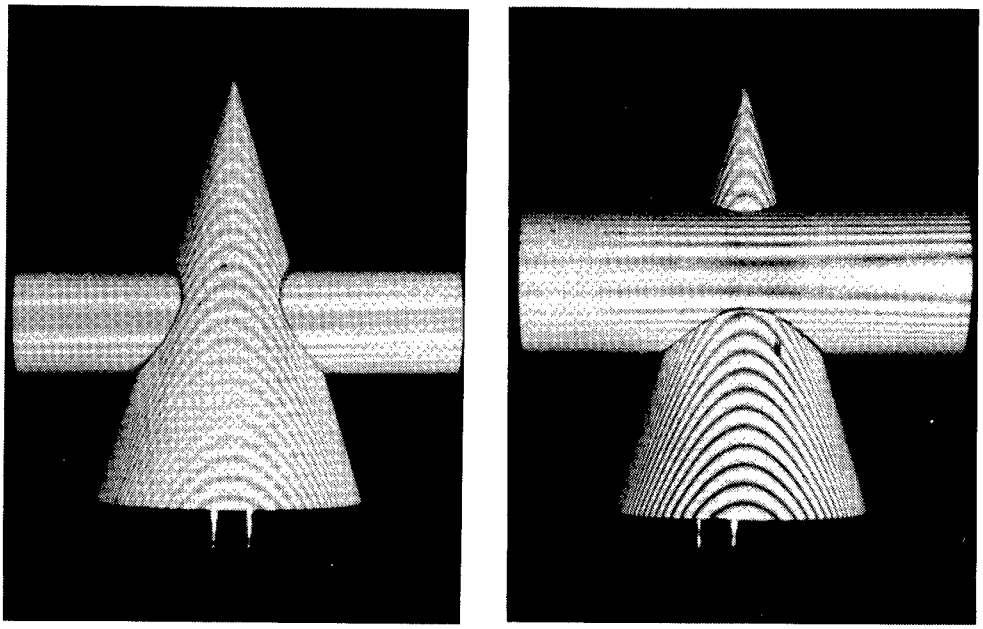

(a) (b)

Photo. 3 Contouring lines of an intersecting bodies, where (a) is a case that a cylinder pierces a cone while (b) is a case that a cone pierces a cylinder. The both cases are free from shadow effects.

declared in Descriptive Geometry[12].

3.2 In Case of Complex Models

Photo. 4 shows a mannequin of living size contoured by the two-source method, where Photo. 4 (a) is by the illumination to have the intensity sum ($I_{S_1} + I_{S_2}$) and the Photo. 4 (b) is by the illumination to yield the intensity multiplication ($I_{S_1} \times I_{S_2}$). The main geometrical parameters are $p_0 = 2$ mm, $d_1 = d_2 = 90$ cm, $h = 189$ cm and $\Delta z = 4.2$ mm. The exposures are about 30 seconds with an ASA 400 film and aperture $f/22$. As seen in Photo. 4, the visibility is better in the latter pattern (b) than in the former one (a). The result will be discussed later in connection with the characteristics of the grating and light source used in the experiment. In general, however, the use of smaller pin holes and more powerful light sources such as an Xe lamp or quartziodine lamp seems to be favarable in order to assure of the enough visibility for the objects of more complex structures. Similar consideration is also essential when the moiré patterns are to be taken of moving objects.

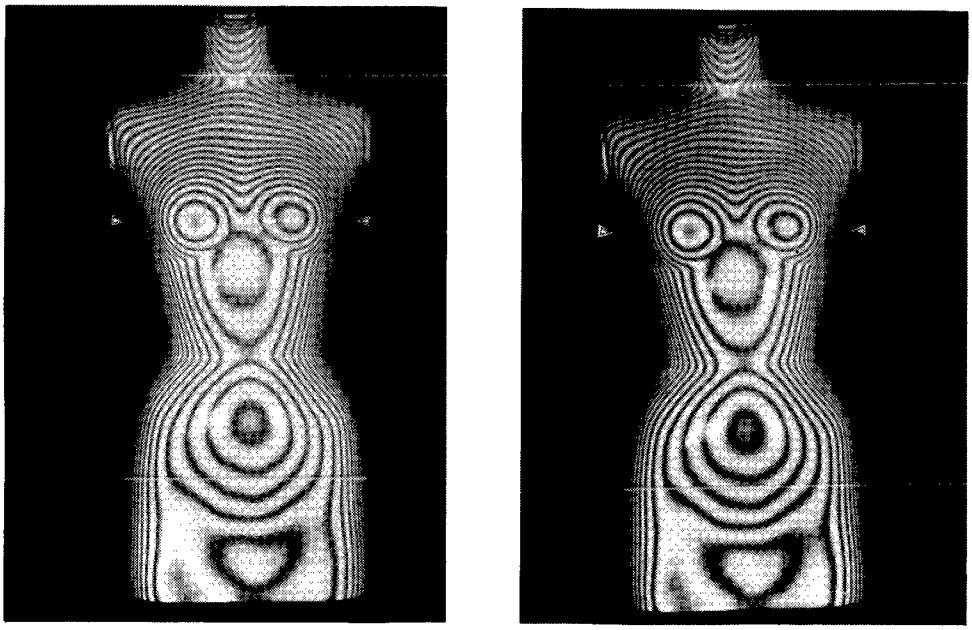

(a) (b)

Photo. 4 Contouring lines of a mannequin of living size, where (a) is by ($I_{S_1} + I_{S_2}$) and (b) is ($I_{S_1} \times I_{S_2}$). The both cases are free from shade and shadow effects.
(▷ mark shows the breast lines where microphotometric scanning was performed.)

4. Discussion and Conclusion

The experiments were mainly performed with the grating made of black nylon strings. The sectional outer shape of the strings can be regarded as a circle, 0.4 mm in radius, and therefore, if the light source is strictly a point source, the light intensity distribution of the projected shade onto the surface of the object should be discribed by a step function, which corresponds to $g(x)$ containing a number of higher harmonics' wave components. In practice, however, the pin hole used as a real light source has an appreciable size, say, 3 mm in diameter, and the edge of the shade of each string becomes dim because of inevitable appearance of the penumbra and partial transparency at the string edge. The situations suggest that the transmittance of the grating may be of the fundamental sine wave.

In order to check the intensity curves predicted in Fig. 2, the two negative photographic films of the moiré patterns shown already in Photo. 4 are scanned along the breast line (shown with ▷ — ◁ marks) with a microphotometer. The intensity distribution curves thus obtained are shown in Fig. 3, where the bias levels for the two films (a) and (b) were adjusted so as to be coincident. Investigating the two curves, the visibility and contrast seem to be better in the film (b), i.e., ($I_{S_1} \times I_{S_2}$) than in the film (a), i.e., ($I_{S_1} + I_{S_2}$), which leads to a conclusion that the grating should behave as a grating of the sinusoidal

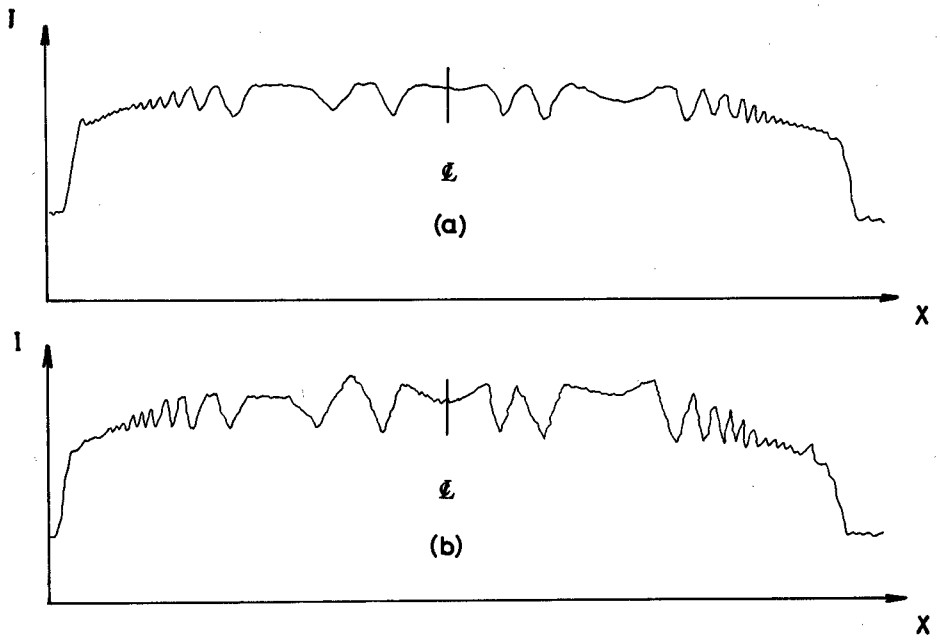

Fig. 3 Intensity curves scanned along the breast lines on the Photo. 4 (a) and (b) with a microphotometer.

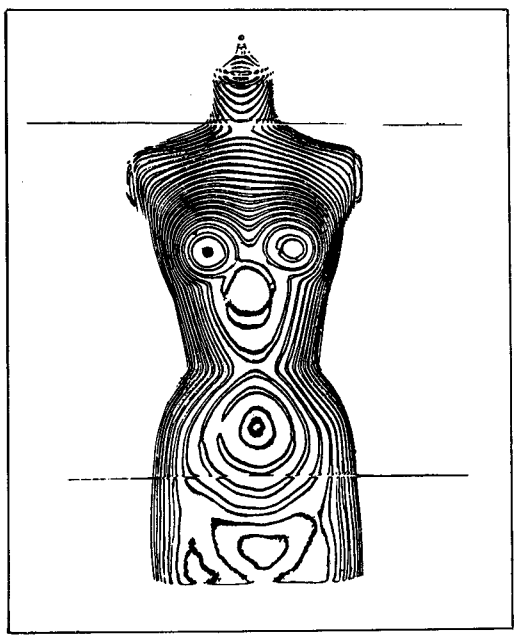

Photo. 5 Contouring lines of a manequin of living size, which was given by intensity multiplication of $(1 - I_{S_1}) \times I_{S_2}$.

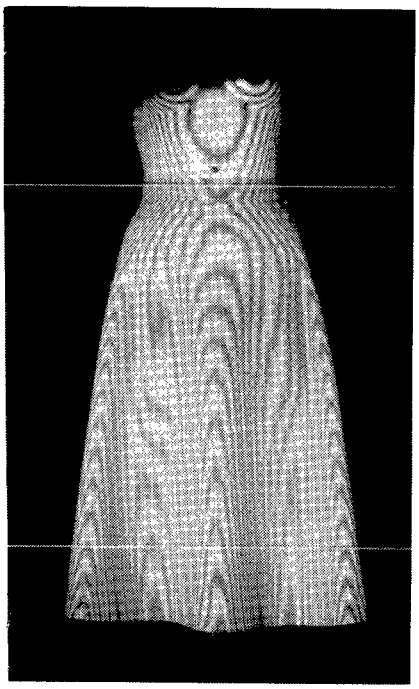

Photo. 6 The moiré topography of a flared skirt having complex curved surface, whose photograph is free from shadow.

form as mentioned above. It should be noted here, that a better contrast and visibility may be obtained if the moiré fringes are constructed by such an intensity multiplication as $(1 - I_{S_1}) \times I_{S_2}$ or $I_{S_1} \times (1 - I_{S_2})$. Photo. 5 is a photograph of this type which was obtained by superimposing a negative film on a positive film instead of using two negative films as in Photo. 4.

Photo. 6 shows a manneqin wearing a skirt as an example of the complex objects, contoured by the present double illumination technique of the intensity sum. Fairly clear shade-free moiré fringes were obtainable even on the part of the skirt, which is of low reflection and has a complex external shape. In this example, the light sources and pin holes are the same as in other observations. As mensioned before, however, smaller pin holes and more powerful light sources may improve visibility and contrast.

In conclusion, the two-source method is effective, to obtain shadow-free moiré pattern from which one can deduce sectional shape of the objects in a practical accuracy and precision.

Acknowledgement

The authors would like to thank Professor S. Fukunaga and Professor R. Nagata of University of Osaka Prefecture for their fruitful discussions and their helpful advices. The authors also would like to thank Professor M. Niwa of Nara Womens' University, and Professor T. Ikuta of Kinki University for the good understandings and the kind suggestions in arranging the experiments.

References

1) D. M. Meadows, W. O. Johnson and J. B. Allen, Appl. Opt. **9**, 942 (1970).
2) H. Takasaki, Appl. Opt. **9**, 1467 (1970).
3) M. Suzuki, M. Kanetani and Y. Suzuki, J. Jap. Soc. of Precision Eng., **40**, 746 (1974).
4) T. Yoshizawa and S. Shimizu, J. Jap. Soc. of Precision Eng., Spring Meeting Pre-Prints 245 (1971).
5) J. D. Hovanesian and Y. Y. Hung, Appl. Opt. **10**, 2735 (1971).
6) H. Takasaki, Appl. Opt. **12**, 845 (1973).
7) Y. Yoshino, M. Tsukiji and H. Takasaki, Appl. Opt. **15**, 2414 (1976).
8) E. Tsutsumi, M. Inomata and M. Komiya, J. of Home Economics of Japan, **31**, 360 (1980).
9) S. Nagae, O. Kinoshita and S. Fukunaga, J. Graphic Science of Japan, **9**, 3 (1971).
10) S. Nagae and S. Fukunaga, J. Graphic Science of Japan, **20**, 7 (1977).
11) S. Nagae, J. Graphic Science of Japan, **25**, 7 (1979).
12) S. Nagae and S. Odaka, J. Graphic Science of Japan, **27**, 3 (1980).